# GSK-3β inhibitor attenuates urinary albumin excretion in type 2 diabetic db/db mice, and delays epithelial-to-mesenchymal transition in mouse kidneys and podocytes

JIA WAN[1,2*], PENG LI[3*], DONG-WEI LIU[2], YING CHEN[4], HAI-ZHEN MO[5], BEN-GUO LIU[5], WEN-JIE CHEN[6], XIAO-QING LU[2], JIA GUO[2], QIAN ZHANG[2], YING-JIN QIAO[2], ZHANG-SUO LIU[2] and GUANG-RUI WAN[3]

[1]Henan Food and Drug Administration, Zhengzhou, Henan 450012; [2]Department of Nephrology, The First Affiliated Hospital of Zhengzhou University, Zhengzhou, Henan 450012; [3]Pharmaceutical College, Xinxiang Medical University, Xinxiang, Henan 453003; [4]School of Life Science and Technology; [5]Department of Food Science, Henan Institute of Science and Technology, Xinxiang, Henan 453003; [6]Modern Education Technology Center, Xinxiang Medical University, Xinxiang, Henan 453003, P.R. China

Received April 10, 2015; Accepted February 2, 2016

DOI: 10.3892/mmr.2016.5441

**Abstract.** The mechanism underlying epithelial-to-mesenchymal transition (EMT) caused by high glucose (HG) stimulation in diabetic nephropathy (DN) remains to be fully elucidated. The present study investigated the effects of HG on EMT and the activity of glycogen synthase kinase 3β (GSK-3β) in podocytes and the kidneys of db/db mice, and assessed the effects of (2'Z, 3'E)-6-bromoindirubin-3'-oxime (BIO), an inhibitor of GSK-3β, on EMT and glomerular injury. The resulting data showed that the activity of GSK-3β was upregulated by HG and downregulated by BIO in the podocytes and the renal cortex. The expression levels of epithelial markers, including nephrin, podocin and synaptopodin, were decreased by HG and increased by BIO, whereas the reverse were true for mesenchymal markers, including α-smooth muscle actin (α-SMA) and fibronectin. The expression levels of β-catenin and Snail, in contrast to current understanding of the Wnt signaling pathway, were increased by HG and decreased by BIO. In addition, expression of the vitamin D receptor (VDR) was decreased by HG and increased by BIO. In conclusion, the present study revealed that the mechanism by which BIO inhibited HG-mediated EMT in podocytes and the renal cortex was primarily due to the VDR. Treatment with BIO protected renal function by maintaining the integrity of the filtration membrane and decreasing UAE, but not by regulating blood glucose. Therefore, GSK-3β may be used as a sensitive biomarker of DN, and its inhibition by BIO may be effective in the treatment of DN.

*Correspondence to:* Dr Zhang-Suo Liu, Department of Nephrology, The First Affiliated Hospital of Zhengzhou University, 1 Jianshe Road, Zhengzhou, Henan 450012, P.R. China
E-mail: zhangsuoliucn@163.com

Mr. Guang-Rui Wan, Pharmaceutical College, Xinxiang Medical University, 601 Jinsui Road, Xinxiang, Henan 453003, P.R. China
E-mail: guangruiwan@yeah.net

*Contributed equally

*Key words:* diabetic nephropathy, epithelial-to-mesenchymal transition, podocytes, glycogen synthase kinase 3β, proteinuria, (2'Z, 3'E)-6-bromoindirubin-3'-oxime, vitamin D receptor

## Introduction

Diabetes mellitus is the leading cause of end-stage renal disease (ESRD), based on the United States renal data system (1). Glycemic control and currently available pharmacotherapies delay, but cannot prevent, the progression of diabetic nephropathy (DN) towards ESRD (2,3). However, in order to develop novel therapies, a full understanding of the etiology of DN is required. Proteinuria, specifically microalbuminuria, is currently one of the earliest clinically identifiable markers of diabetes-induced renal damage, and the likelihood of progression to ESRD is significantly correlated with the level of albuminuria (4-7). Proteinuria not only predicts the speed of development in ESRD, but also correlates with renal decline. In addition, patients with DN with low levels of proteinuria have a markedly slower rate of disease progression, compared with those with a high rate of urinary protein excretion (8-11). The selection of targets and the timing of intervention are, thus critical for effectively preventing DN. Therefore, identifying the appropriate cellular targets for therapeutic intervention is crucial to enable the prevention of proteinuria. The progression of DN frequently begins with injury to podocytes, and there is a close association between the onset of albuminuria and podocytopathies (12,13), including foot process effacement, podocyte hypertrophy, detachment, apoptosis and epithelial-to-mesenchymal transition (EMT) (14). Based on various human and experimental models, DN is associated with a decreased number of podocytes per glomerulus and foot process effacement upon biopsy (15). Previous studies in OVE26 transgenic mice, a model of type-1 DN, demonstrated

that reduced podocyte numbers and density frequently follow the onset of micro-albuminuria and more subtle podocyte injuries (16,17). Therefore, podocyte effacement and loss are critical events in the early progression of DN.

The EMT can also result in podocyte loss, during which epithelial cells undergo morphological changes. Podocyte EMT can be caused by the loss of epithelial P-cadherin, zonula occludens-1 or nephrin, and additional stimuli include the acquisition of mesenchymal FspI, desmin, collagen I and fibronectin (18). Podocytes can also undergo EMT under conditions of high glucose (19), which is associated with increased podocyte detachment, microalbuminuria and more severe glomerular pathology. Several intracellular signaling pathways regulate EMT, including transforming growth factor-β/small mothers against decapentaplegic, Wnt/β-catenin and integrin-linked kinase (ILK) (20). Glycogen synthase kinase 3β (GSK-3β) is involved in all these pathways, and thus may be pivotal in podocyte EMT (20). Therefore, GSK-3β inhibitors have been investigated in mesangial proliferative glomerulonephritis, crescent glomerulonephritis and lupus nephritis (21). In these studies, the GSK-3β inhibitor, (2'Z, 3'E)-6-bromoindirubin-3'-oxime (BIO), was found to inhibit high glucose-stimulated apoptosis in mesangial cells.

The mechanisms involved in glomerular injury and proteinuria during diabetes mellitus require additional investigation. The present study investigated the association between high glucose and EMT in podocytes and in the kidneys of db/db diabetic mice. In addition, the present study investigated the therapeutic potential of modulating GSK-3β and EMT, in the presence of high glucose, for DN.

## Materials and methods

*Animals*. The Committee for the Care and Use of Laboratory Animals of Xinxiang Medical College (Xinxiang, China) approved all animal experiments. A total of 48 male db/db mice and 24 age-matched db/+ control mice were selected (Model Animal Research Center of Nanjing University, Nanjing, China). At an age of 12 weeks, the db/+ mice (normal control group; NC) and 24 db/db mice (diabetic nephropathy group; DN) were subcutaneously injected with dimethyl sulfoxide used as a diluent (Sigma-Aldrich, St. Louis, MO, USA), whereas the remaining 24 db/db mice (BIO intervention group; BIO) were injected with 320 μg/kg per day BIO (Sigma-Aldrich). All mice were housed in temperature- and humidity-controlled IVC-II independent supply isolation cages (Jinan Aonuo CNC Equipment Co., Ltd., Jinan, China), with free access to pure water and standard laboratory chow. When the mice were 12, 15 and 18 weeks old, eight mice in each group were sacrificed. On the day prior to sacrifice, the mice were individually housed in metabolic cages for the collection of urine over 24 h. The levels of urinary albumin excretion (UAE) were quantified using an albumin ELISA kit (Abcam, Cambridge, MA, USA). Heart blood (1 ml) was drawn and centrifuged at 625 x g at 4˚C for 4 min. Serum glucose was measured at the time of sacrifice using an automatic analyzer (SPOTCHEM EZ SP-4430; ARKRAY, Inc., Kyoto, Japan). Following sacrifice of the mice, the kidneys were rapidly dissected and weighed, and the cortices were separated. Renal tissue sections (4 μm) were prepared and stained with hematoxylin and eosin (HE; Fuzhou Maixin Biotechnology Development Co., Ltd., Fuzhou, China), followed by assessment using light microscopy (Leica Microsystems GmbH, Wetzlar, Germany). In addition, electron microscopy was used to observe the micro-morphological changes in the renal tissues. A total of 20 glomeruli were evaluated for each mouse. The present study was approved by the ethics committee of the First Affiliated Hospital of Zhengzhou University (Zhengzhou, China).

*Cell culture and treatment*. Cells of the MPC-5 clonal cell line of conditionally immortalized mouse podocytes, cultured *in vitro* from H-2Kb-tsA58 mice, were provided by American Mount Sinai Medical College, and were cultured, as previously described (22). For propagation, the cells were cultured at 33˚C in RPMI 1640 medium (Gibco; Thermo Fisher Scientific, Inc., Waltham, MA, USA) supplemented with 10 U/ml mouse recombinant interferon-γ (Shanghai Sangon Biological Engineering Technology and Services, Co., Ltd., Shanghai, China) and 10% fetal bovine serum (Invitrogen; Thermo Fisher Scientific, Inc.) to enhance the expression of a thermosensitive T antigen. The cells were then grown under non-permissive conditions at 37˚C, without interferon-γ, for 14 days to induce differentiation. The podocytes were then cultured with or without high glucose (25 mmol/l; Sigma-Aldrich), in the presence or absence of BIO (10 μmol/l) for 36 h.

*Electron microscopy (EM)*. Samples from 24 mice were used for the EM. Following anesthesia with ketamine (100 mg/kg; Sigma-Aldrich), the mice were sacrificed by cervical dislocation and 2% glutaraldehyde was perfused into the kidneys, which were then excised and immersed in the same fixative overnight. The tissue blocks were then fixed in 2% osmium tetroxide (Sigma-Aldrich) for 2 h at 4˚C, dehydrated using an ethanol gradient and Epon-embedded (Fuzhou Maixin Biotechnology Development Co., Ltd.). Ultrathin sections (80 nm) stained with 4% uranyl acetate (Sigma-Aldrich) and with 1% lead citrate (Sigma-Aldrich), were cut using an ultra-microtome (EM UC7; Leica Microsystems GmbH) and examined by EM (JEM-100SX; JEOL, Ltd., Tokyo, Japan).

*Western blotting*. Western blotting was performed using established protocols to assess specific protein expression levels, as previously described (23). Radioimmunoprecipitation assay lysis buffer (Santa Cruz Biotechnology, Inc., Dallas, TX, USA) according to the manufacturer's protocols, and protein concentration was determined using the Coomassie brilliant blue method. Proteins (30 μg) were separated on 10% SDS-PAGE gels for 3 h, then transferred to polyvinylidene fluoride membranes. Following washing with phosphate-buffered saline three times for 14 min, 1% bovine serum albumin (Fuzhou Maixin Biotechnology Development Co., Ltd.) was used to block the membrane for 2 h. Following blocking, the membranes were incubated with primary antibodies overnight at 4˚C as follows: Rabbit polyclonal anti-podocin (dilution, 1:1,000; Bioss, Inc., Woburn, MA, USA; cat. no. bs6597R) rabbit polyclonal anti-nephrin (dilution, 1:1,000; cat. no. ab58968), rabbit polyclonal anti-synaptopodin (dilution, 1:200; cat. no. ab109560), rabbit

Table I. Primer sequences, product sizes and annealing temperatures/durations for reverse transcription-quantitative polymerase chain reaction analysis.

| Gene | Primer sequence | Product (bp) | Duration (sec) | Temp (˚C) |
|---|---|---|---|---|
| GAPDH | F: 5'-CCTGCACCACCAACTGCTTAGC | | | |
| | R: 5'-CCAGTGAGCTTCCCGTTCAGC | 238 | 30 | 56 |
| Nephrin | F: 5'-CCCAGGTACACAGAGCACAA | | | |
| | R: 5'-CTCACGCTCACAACCTTCAG | 200 | 30 | 55 |
| α-SMA | F: 5'-TACTGCCGAGCGTGAGA | | | |
| | R: 5'-GCTTCGTCGTATTCCTGTTT | 489 | 30 | 51 |
| GSK-3β | F: 5'-TTCAGGCCGCTGTTCACCG | | | |
| | R: 5'-GTGCTGGTCTTTCCCGCGCA | 152 | 30 | 60 |
| β-catenin | F: 5'-CTCATTCCACCAACTGCTTGGC | | | |
| | R: 5'-TAAGTGAGCTTTCGGTTCAGC | 298 | 30 | 51 |
| Snail | F: 5'-CCCTAGGTACACAGAGCACG | | | |
| | R: 5'-GCCACGCTCACAACCTTACG | 408 | 30 | 54 |

α-SMA, α-smooth muscle actin; GSK-3β, glycogen synthase kinase 3β; F, forward; R, reverse.

polyclonal anti-α-SMA (dilution, 1:400; cat. no. ab5694), rabbit polyclonal anti-fibronectin (dilution, 1:2,000; cat. no. ab2413), rabbit polyclonal anti-phosphorylated-Tyr$^{216}$-GSK-3β (dilution, 1:1,000; cat. no. ab75745), mouse polyclonal anti-vitamin D receptor (VDR; dilution, 1:1,000; cat. no. ab3508), and mouse monoclonal anti-β-actin (dilution, 1:1,000; cat. no. ab6276), mouse monoclonal anti-GSK-3β (dilution, 1:1,000; cat. no. ab75745; all from Abcam), rabbit monoclonal anti-phosphorylated-Ser$^{9}$-GSK-3β (dilution, 1:1,000; cat. no. 5558), rabbit monoclonal anti-β-catenin (dilution, 1:1,000; cat. no. 8480), rabbit monoclonal anti-Snail (dilution, 1:1,000; cat. no. 3879; all from Cell Signaling Technology, Inc., Danvers, MA, USA). The secondary antibodies used incubated with the membrane for 2 h at room temperature and were as follows: alkaline phosphatase-labeled goat anti-rabbit IgG (dilution l:200; Abcam; cat. no ab97048) and alkaline phosphatase-labeled horse anti-mouse IgG (dilution l:200; Vector Laboratories, Inc., Burlingame, CA, USA; cat. no. AP-2000), goat anti-rabbit IgG (dilution l:200; Abcam; cat. no. ab6721) and donkey anti-mouse IgG (dilution l:300; Abcam; cat. no. ab150105). Visualization was performed using nitro-blue tetrazolium/5-bromo-4-chloro -3'-indolyphosphate coloration (Wuhan Boster Biological Technology, Ltd., Wuhan, China). The intensities of the bands were measured and quantified using ImageJ analysis software (version 1.46; imagej.nih.gov/ij/).

*Reverse transcription-quantitative polymerase chain reaction (RT-qPCR) analysis*. Total RNA was isolated using TRIzol reagent (Invitrogen; Thermo Fisher Scientific, Inc.), according to the manufacturer's protocol. Synthesis of the first strand of cDNA was performed in 20 $\mu$l reaction buffer with 2 $\mu$g (13 $\mu$l) RNA, 4 $\mu$l 5X PrimeScript Buffer (Takara Biotechnology, Co., Ltd., Dalian, China), 1 $\mu$l PrimeScript RT Enzyme mix (Takara Biotechnology, Co., Ltd.), 1 $\mu$l Oligo-dT primer (50 $\mu$mol/l) and 1 $\mu$l random hexamers (100 $\mu$mol/l) at 37˚C for 15 min, followed by 85˚C for 5 sec. qPCR was performed, according to standard protocols with 3 $\mu$l aliquots of cDNA (5 ng/$\mu$l) using specific primer pairs, the sequences of which are shown in Table I. The reaction mixture (15 $\mu$l) contained 7.5 $\mu$l 2X Premix Ex Taq (Takara Biotechnology, Co., Ltd.), 0.25 $\mu$l (10 $\mu$mol/l) forward primer, 0.25 $\mu$l (10 $\mu$mol/l) reverse primer, 3 $\mu$l cDNA and 4 $\mu$l distilled water and the PCR reaction was performed in a Veriti® 96-Well Thermal Cycler (Applied Biosystems; Thermo Fisher Scientific, Inc.). Following an initial denaturation at 95˚C for 3 min, the thermocycling conditions were as follows: For nephrin, 40 cycles of 95˚C for 30 sec, 56˚C for 30 sec and 72˚C for 1 min, followed by 72˚C for 5 min; for α-SMA, 40 cycles of 95˚C for 30 sec, 52˚C for 30 sec and 72˚C for 1 min, followed by 72˚C for 5 min; for GSK-3β, 40 cycles of 95˚C for 30 sec, 59˚C for 30 sec and 72˚C for 1 min, followed by 72˚C for 5 min; for Snail, 40 cycles of 95˚C for 30 sec, 55˚C for 30 sec and 72˚C for 1 min, followed by 72˚C for 5 min; for β-catenin, 45 cycles of 95˚C for 30 sec, 51˚C for 30 sec and 72˚C for 1 min, followed by 72˚C for 5 min; and for GAPDH, 40 cycles of 95˚C for 30 sec, 60˚C for 30 sec and 72˚C for 1 min, followed by 72˚C for 5 min. ImageJ software was used to visualize the qPCR product sizes fractionated on a 1.0% agarose gel (Sigma-Aldrich).

*GSK-3β kinase activity*. The activity of GSK-3β was assayed using a GSK-3β Activity assay kit (Sigma-Aldrich), according to the manufacturer's protocol and as previously described (24). Activity was calculated following determining optical densities (OD) using the following formula: GSK-3β activity = [(OD sample - OD blank) x 0.1 x gradient concentration] / 0.005 x 6.22 x 5.

*Statistical analysis*. All data are presented as the means ± standard deviation of three independent experiments and statistical analysis was conducted using SPSS 17.0 software (SPSS, Inc., Chicago, IL, USA). The physiological variables were analyzed using one-way analysis of variance

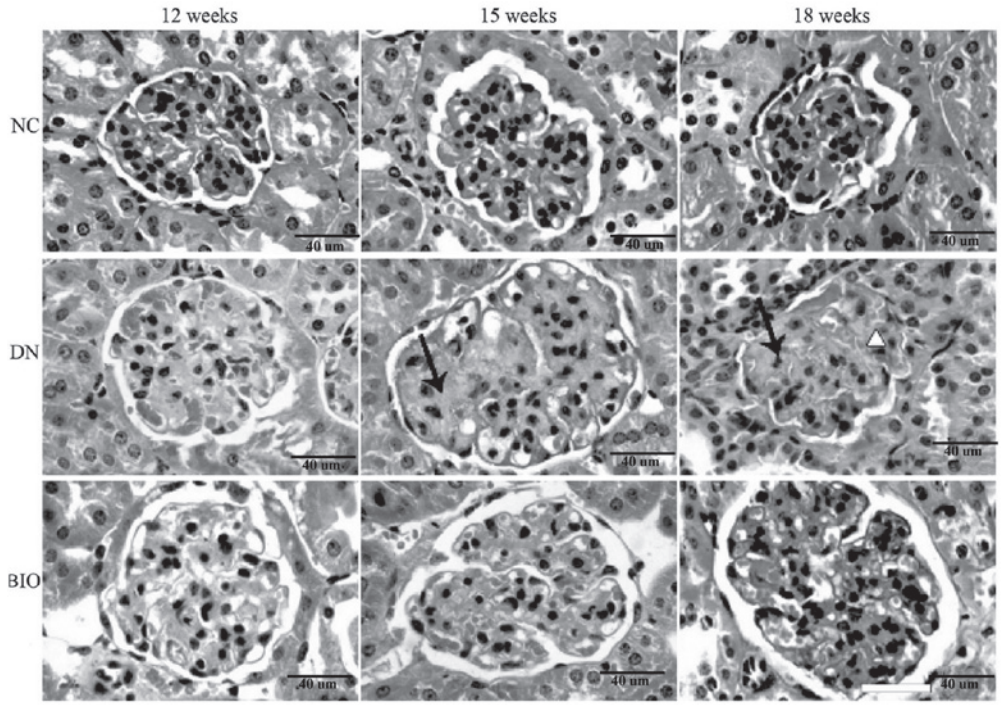


Figure 1. HE staining of mouse kidney sections in the NC, DN and BIO groups at 12, 15 and 18 weeks of age. Kidney sections were harvested from mice in the NC, DN and BIO groups at 12, 15 and 18 weeks-of-age, and were stained with HE. The DN group exhibited increased mesangial matrix, adhesion of balloon loops and Baumann's capsule walls at 12 weeks, and the effects were more prominent by 18 weeks-of-age, compared with the mice in NC group. Following treatment with BIO for 6 weeks (from 12 weeks of age), there was a significant decrease in mesangial matrix in and the number and extent of glomerular sclerosis, compared with the untreated DN mice. Arrows indicate Kimmelstiel-Wilson nodules. Triangles indicate adhesion of balloon loops and Baumann's capsules. Scale bar=40 $\mu$m (n=8). HE, hematoxylin and eosin; NC, normal control (db/+); DN, diabetic neuropathy (db/db); BIO, (2'Z, 3'E)-6-bromoindirubin-3'-oxime-treated.

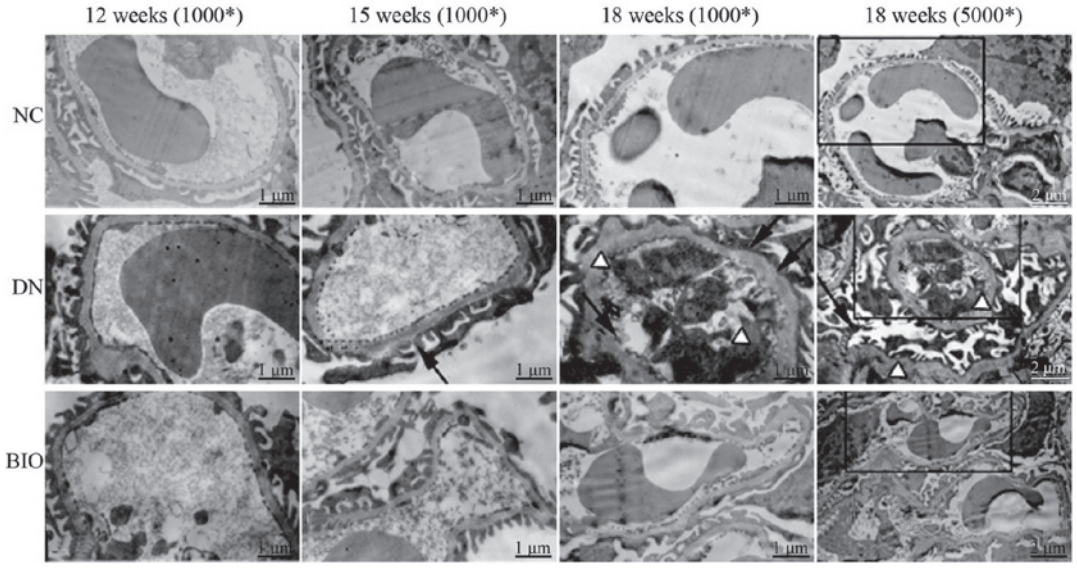


Figure 2. Ultrastructural examination using transmission electron microscopy in the NC, DN and BIO groups at 12, 15 and 18 weeks of age. Ultrathin sections (80 nm) were harvested from mice in the NC, DN and BIO groups at 12, 15 and 18 weeks-of-age, and were stained with 4% uranyl acetate and 1% lead citrate. Fusion and loss of foot processes, and increase in the thickness of the GBM were found in the DN group, compared with the NC group. Following treatment with BIO for 6 weeks (from 12 weeks of age), there was a significant decrease in foot process fusion and GBM thickness, compared with the DN group. The black boxes on the images at 18 weeks show the area of the image, which was magnified by 200% and shown to its left. White arrowheads indicate foot process effacement of podocytes; triangle indicate thickening of the GBM (n=8). NC, normal control group (db/+); DN, diabetic neuropathy group (db/db); BIO, (2'Z, 3'E)-6-bromoindirubin-3'-oxime-treated DN group; GBM, glomerular basement membrane.

followed by least significant difference multiple comparison post-hoc analysis. Other variables were compared using a Kruskal-Wallis non-parametric test followed by multiple comparisons using Duncan's method. For all comparisons, $P<0.05$ was considered to indicate a statistically significant difference.

Table II. Effects of BIO on blood glucose, UAE, bodyweight, and kidney weight.

| | Time point (age of mice) | | | | |
|---|---|---|---|---|---|
| | 12 weeks | 15 weeks | 18 weeks | F-value | P-value |
| Blood glucose (mmol/l) | | | | | |
| NC group | 6.11±1.02 | 6.18±0.99 | 6.29±0.54 | 0.129 | 0.880 |
| DN group | 27.50±7.78[a] | 28.03±7.91[a] | 28.90±7.18[a] | 0.222 | 0.804 |
| BIO group | 27.24±7.08[a] | 28.29±4.57[a] | 28.77±2.71[a] | 0.502 | 0.523 |
| F value | 32.368 | 45.797 | 68.606 | - | |
| P-value | <0.05 | <0.05 | <0.05 | - | - |
| Urinary albumin excretion ($\mu$g/24 h) | | | | | |
| NC group | 36.15±7.18 | 38.39±7.24 | 39.39±4.46 | 1.466 | 0.264 |
| DN group | 239.24±37.80[a] | 244.66±35.30[a,c] | 285.41±28.41[a,c] | 44.826 | <0.05 |
| BIO group | 239.54±24.08[a] | 182.51±19.05[a-c] | 135.65±18.96[a-d] | 182.992 | <0.05 |
| F value | 160.420 | 161.764 | 310.919 | - | - |
| P-value | <0.05 | <0.05 | <0.05 | - | - |
| Body weight (g) | | | | | |
| NC group | 11.96±1.02 | 14.54±1.19 | 16.06±1.27 | 62.437 | <0.05 |
| DN group | 29.91±4.71[a] | 34.24±4.08[a] | 36.95±5.23[a] | 30.326 | <0.05 |
| BIO group | 29.93±4.85[a] | 32.09±4.93[a,b] | 32.49±4.77[a,b] | 3.664 | 0.052 |
| F value | 55.200 | 66.077 | 56.106 | - | - |
| P-value | <0.05 | <0.05 | <0.05 | - | - |
| Kidney weight (mg) | | | | | |
| NC group | 107.32±8.77 | 116.02±8.82 | 123.92±7.24 | 96.946 | <0.05 |
| DN group | 180.00±25.66[a] | 189.95±19.27[a,c] | 197.41±17.53[a,c] | 8.318 | <0.05 |
| BIO group | 180.78±14.97[a] | 174.58±16.28[a,b,c] | 159.90±22.53[a-d] | 16.383 | <0.05 |
| F value | 44.514 | 51.124 | 37.360 | - | - |
| P-value | <0.05 | <0.05 | <0.05 | - | - |

[a]P<0.05, vs. NC group at same time point; [b]P<0.05, vs. DN group at same time point. [c]P<0.05, vs. in same treatment group at 12 weeks. [d]P<0.05, vs. same treatment group at 15 weeks (n=8). NC, normal control (db/+); DN, diabetic neuropathy (db/db); BIO, (2'Z, 3'E)-6-bromoindirubin-3'-oxime-treated.

## Results

*Effects of BIO on blood glucose, UAE, body weight and kidney weight*. As summarized in Table II, blood glucose remained significantly elevated in the DN and BIO groups, compared with the NC group throughout the experiment. No significant differences were found between the DN and BIO groups, suggesting that BIO had no effect on blood glucose. The levels of UAE increased from the age of 12 weeks, and continued to increase until the age of 18 weeks. The increases in UAE were predominantly attenuated in the BIO-treated mice, compared with the DN mice, suggesting that BIO inhibited damage to the glomerular filtration membrane. The body and kidney weights were also increased by 12 weeks of age, and continued to increase at 15 and 18 weeks. The increases in body weight and kidney weight were markedly lower in the BIO group, compared with the DN group. These data suggested that BIO significantly attenuated DN.

*Kidney morphology*. Following staining with HE, the renal cortices were observed under a light microscope. Compared with the NC group (Fig. 1A-C), increases in the mesangial matrix, occlusion of kidney tubules, sclerosis of the glomerulus, adhesion of balloon loops and Baumann's capsule walls were observed when the DN mice were 12 weeks old, and became more prominent by 18 weeks (Fig. 1D-F). These changes were significantly attenuated in the BIO group, compared with the DN group (Fig. 1G-I). Compared with the NC group (Fig. 2A-D), fusion and loss of foot processes, increased thickness of the glomerular basement membrane (GBM), increased mesangial matrix and collagen fiber, and hyaline degeneration of afferent and efferent vessels were detected in the DN mice (Fig. 2E-H). These changes were also significantly attenuated in the BIO group, compared with the DN group, suggesting that BIO slowed down the pathological changes in the glomerulus stimulated by DN (Fig. 2I-L).

*Effects of BIO on the expression of epithelial cell markers*. The expression levels of phenotypic markers for epithelial cells in mouse kidney tissues were compared, with β-actin as a loading control, using Western blotting and RT-qPCR analysis. With the progression of DN, the expression of nephrin decreased

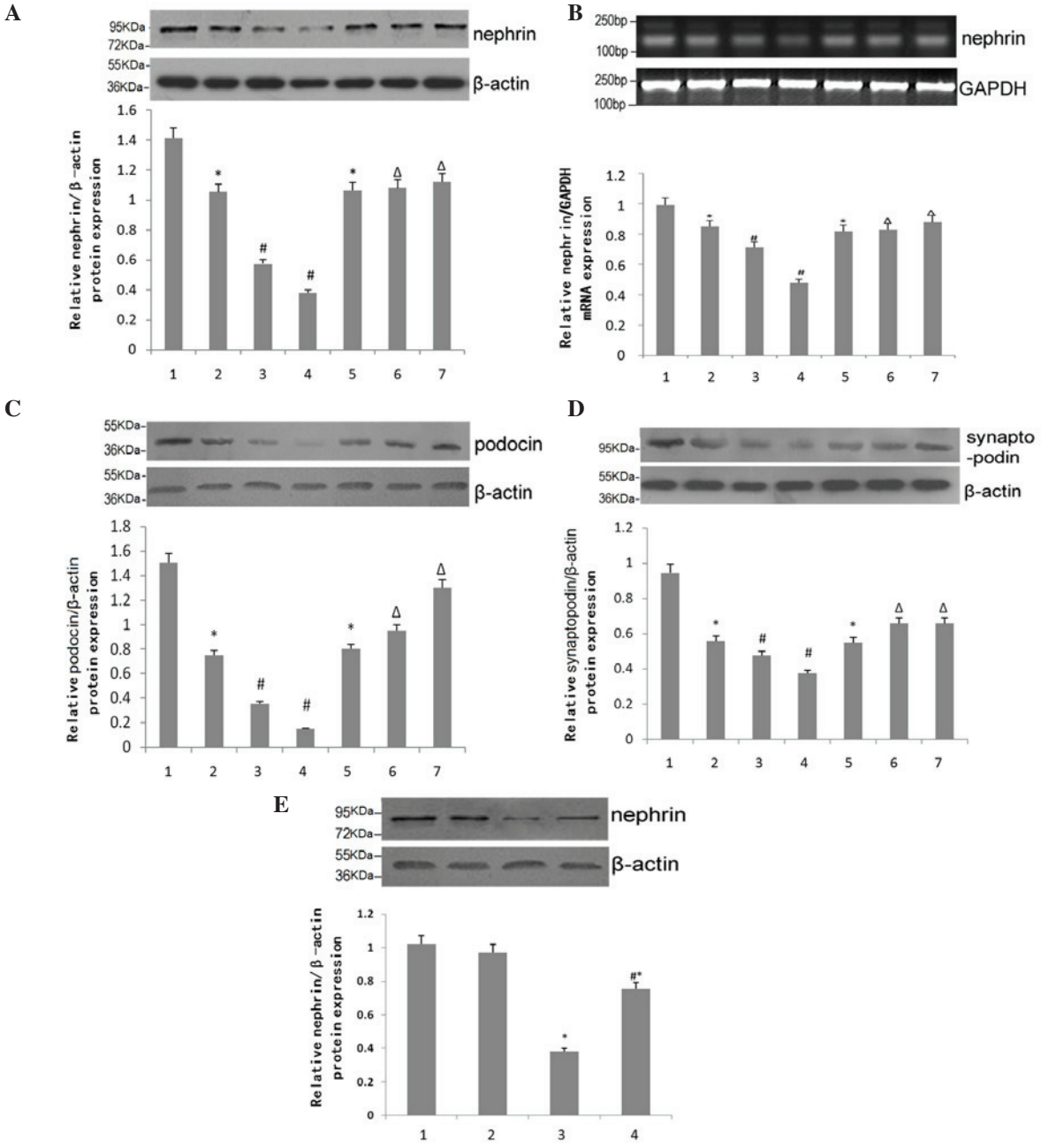


Figure 3. Effect of BIO on the expression of epithelial cell markers. (A) Western blotting for the expression of nephrin in kidneys of NC, DN and DN+BIO mice. Data are presented as the mean ± standard error of the mean (n=6). (B) Reverse transcription-quantitative polymerase chain reaction analysis for the mRNA expression of nephrin in the kidneys of NC, DN and DN+BIO mice. Data are presented as the mean ± standard error of the mean (n=6). (C and D) Western blotting for the protein expression of podocin in the kidneys of NC, DN and DN+BIO mice. Data are presented as the mean ± standard error of the mean (n=3). 1, NC group; 2, DN group; 3, 15 week DN group; 4, 18 week DN group; 5, 12 week BIO group; 6, 15 week BIO group; 7, 18 week BIO group. (E) Western blotting for the protein expression of nephrin in the kidneys of NC, DN and DN+BIO mice. Data are presented as the mean ± standard error of the mean (n=4). 1-4: 1, normal glucose without BIO; 2, normal glucose with BIO; 3, high glucose without BIO; 4, high glucose with BIO. $^{*}$P<0.05. vs. mice in NC group, or podocytes in the normal glucose group without BIO; $^{\#}$P<0.05, vs. 12-week-old mice in the DN group, or podocytes in the high glucose group without BIO treatment; $^{\Delta}$P<0.05, vs. 12-week-old mice in the DN+BIO group. NC, normal control group (db/+); DN, diabetic neuropathy group (db/db); BIO, (2'Z, 3'E)-6-bromoindirubin-3'-oxime.

significantly in the DN group (Fig. 3). However, nephrin levels were significantly attenuated at 15 and 18 weeks of age in the BIO group, compared with the DN group (Fig. 3A). The results of the RT-qPCR analysis of mRNA levels of nephrin in mouse kidney tissue were analyzed using ImageJ software, which confirmed these observations (Fig. 3B). Similar expression patterns were observed in the protein expression levels of podocin and synaptopodin, two other epithelial markers (Fig. 3C and D).

The expression levels of nephrin in podocytes exposed to high or normal glucose, treated with or without BIO were compared. BIO had no effect under normal glucose conditions (Fig. 3A; P>0.05). Under conditions of high glucose, the expression of nephrin in the podocytes was significantly reduced, compared with the normal glucose group (P<0.05). However, treatment with BIO partially alleviated the high glucose-mediated reduction in the expression of nephrin

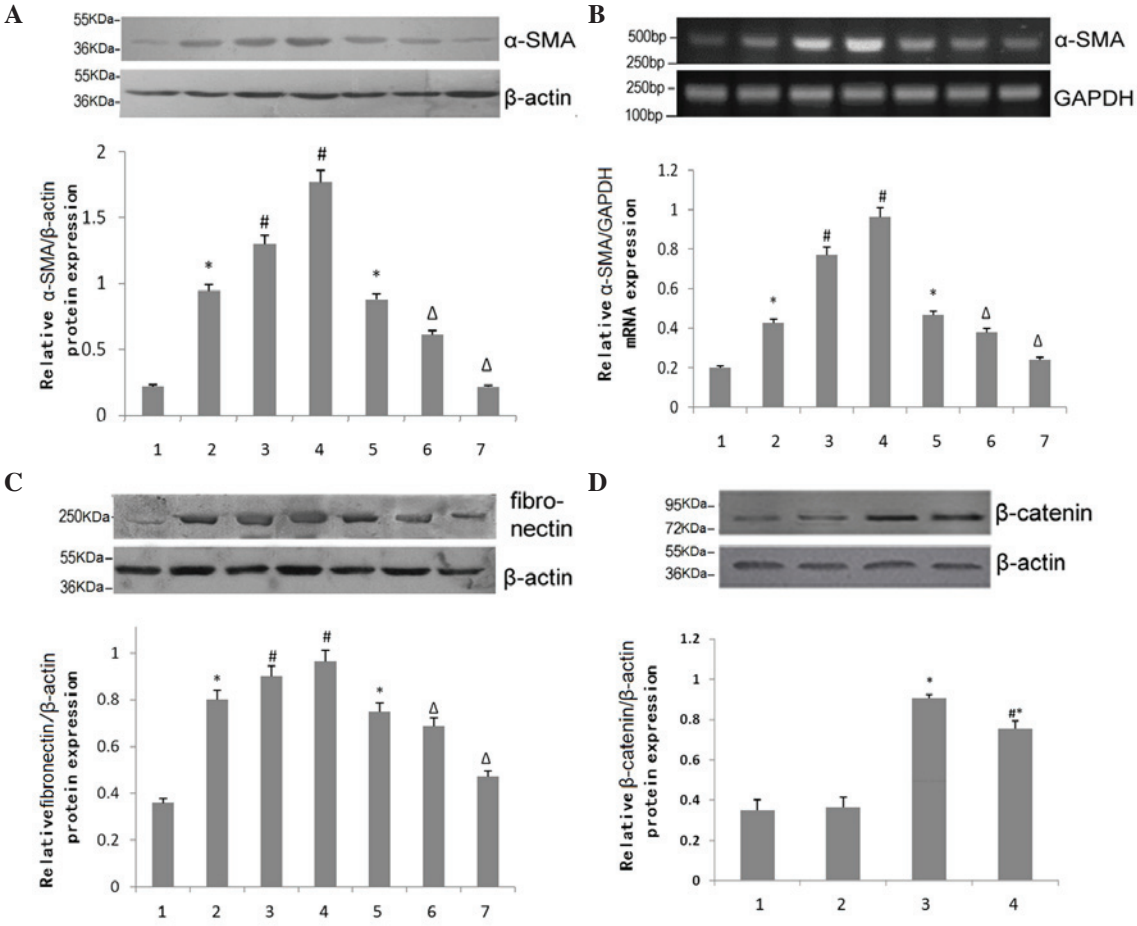


Figure 4. Effect of BIO on the expression levels of mesenchymal cell markers. (A) Western blotting for the expression of α-SMA in the kidneys of NC, DN and DN+BIO mice. Data are presented as the mean ± standard error of the mean (n=6). (B) Reverse transcription-quantitative polymerase chain reaction analysis for the mRNA expression of α-SMA in the kidneys of NC, DN and DN+BIO mice. Data are presented as the mean ± standard error of the mean (n=6). (C) Western blotting for the expression of fibronectin in the kidneys of NC, DN and DN+BIO mice. Data are presented as the mean ± standard error of the mean (n=4). 1, NC group; 2, DN group; 3, 15 week DN group; 4, 18 week DN group; 5, 12 week BIO group; 6, 15 week BIO group; 7, 18 week BIO group. (D) Western blotting for the expression of β-catenin in podocytes in high or normal glucose, with and without BIO treatment. Data are presented as the mean ± standard error of the mean (n=5). 1-4: 1, normal glucose without BIO; 2, normal glucose with BIO; 3, high glucose without BIO; 4, high glucose with BIO. $^{*}$P<0.05, vs. mice or podocytes in NC group. $^{\#}$P<0.05, vs. 12-week-old mice in the DN group or podocytes in the high glucose group without BIO treatment; $^{\Delta}$P<0.05, vs. 12-week-old mice in the BIO group. α-SMA, α-smooth muscle actin; NC, normal control group (db/+); DN, diabetic neuropathy group (db/db); BIO, (2'Z, 3'E)-6-bromoindirubin-3'-oxime.

(P<0.05), but did not restore expression levels to normal (P<0.05).

*Effects of BIO on the expression of mesenchymal cell markers.* The protein expression of mesenchymal cell phenotypic markers in the mouse kidney were normalized to β-actin, as an internal reference, for RT-qPCR analysis. As DN progressed, the expression of α-SMA in the DN group increased significantly in a time-dependent matter. However, these effects were attenuated at 15 and 18 weeks of age in the BIO group, compared with the DN group (Fig. 4A). RT-qPCR analysis of α-SMA in the kidneys of 15-week-old mice quantitatively confirmed these observations, as analyzed using ImageJ software (Fig. 4B). Similar expression patterns of fibronectin, another mesenchymal cell marker, were observed (Fig. 4C).

The expression levels of α-SMA in podocytes under conditions of high or normal glucose, with or without BIO treatment were then compared (Fig. 4D). Treatment with BIO had no effect on the expression of α-SMA under normal glucose concentrations (P>0.05). However, the expression of α-SMA was increased significantly under high-glucose conditions, compared with normal glucose (P<0.05). Treatment with BIO partially alleviated the high glucose-induced increase in the expression of α-SMA (P<0.05), but did not restore expression levels to normal (P<0.05).

*Effects of BIO on the expression and activity of GSK-3β.* GSK-3β, which is constitutively expressed in all eukaryotic cells, is a serine/threonine kinase. The important regulatory amino acids are Tyr-216 for activation and Ser-9 for inhibition. The expression levels of total-GSK-3β in the mouse kidney tissues were compared, with β-actin as a loading control, using RT-qPCR analysis. As DN progressed, the expression of total-GSK-3β in the DN group increased significantly in a time-dependent matter (P<0.05). However, total-GSK-3β levels were substantially attenuated at 15 and 18 weeks of age in the BIO group, compared with the DN group (P<0.05; Fig. 5A). ImageJ software was used to quantify the mRNA expression of GSK-3β in the mouse kidney following RT-qPCR analysis. The data from the animals at 15 weeks of age were consistent with

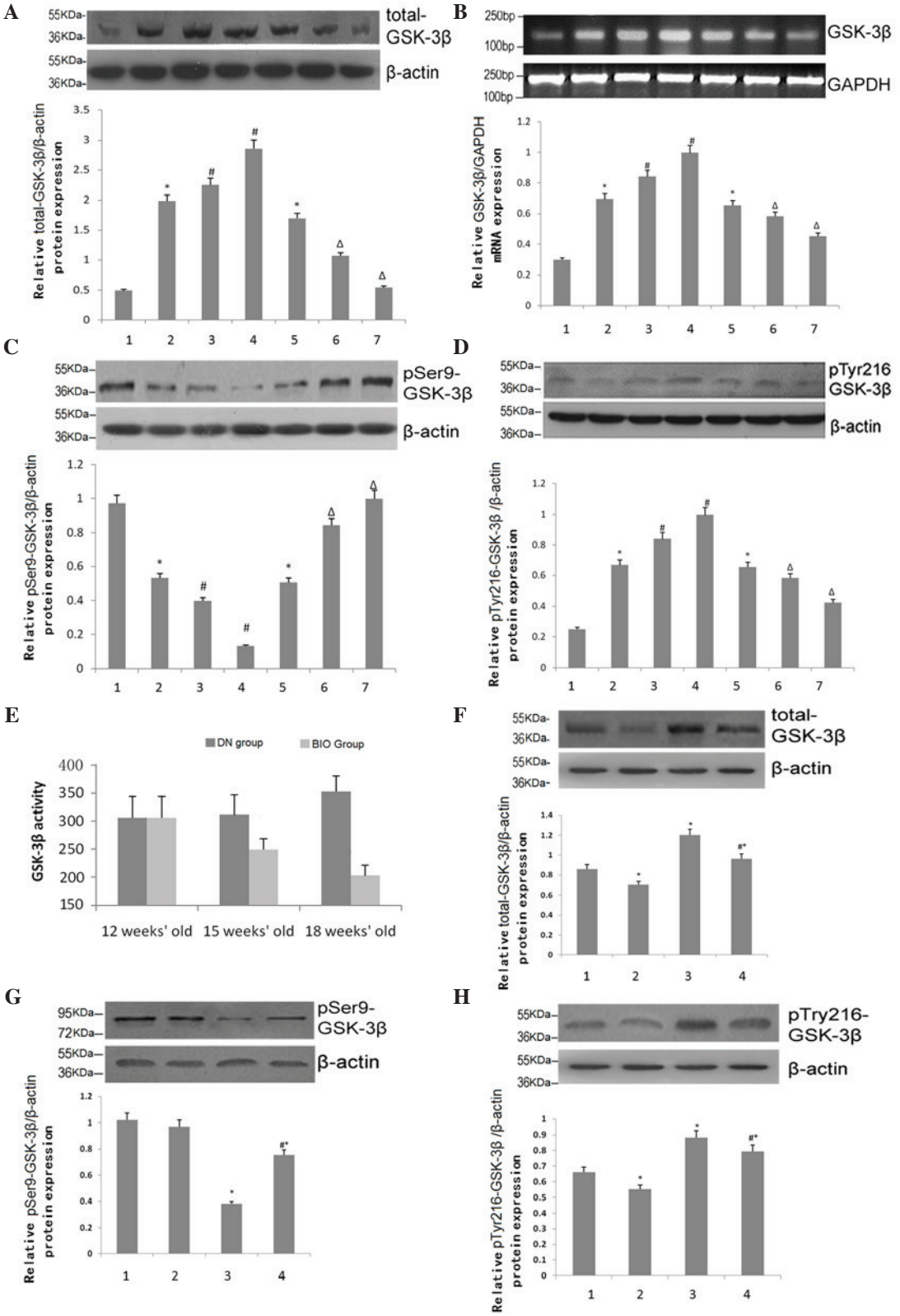


Figure 5. Effects of BIO on the expression and activity of GSK-3β. (A) Western blotting for the protein expression of total-GSK-3β in the kidneys of NC, DN and DN+BIO mice (n=4). (B) Reverse transcription-quantitative polymerase chain reaction analysis of mRNA expression of GSK-3β in the kidneys of NC, DN and DN+BIO mice (n=6). (C) Western blotting for pSer9-GSK-3β expression in the kidneys of NC, DN and DN+BIO mice (n=4). (D) Western blotting for the expression of pTyr216-GSK-3β in the kidneys of NC, DN and DN+BIO mice (n=4). 1, NC group; 2, DN group; 3, 15 week DN group; 4, 18 week DN group; 5, 12 week BIO group; 6, 15 week BIO group; 7, 18 week BIO group. (E) Kinase activity of GSK-3β in the kidneys of NC, DN and DN+BIO mice. (F) Western blotting for the protein expression of total-GSK-3β in podocytes in high or normal glucose, with and without BIO treatment (n=5). (G) Western blotting for the protein expression of pSer9-GSK-3β in podocytes in high or normal glucose, with and without BIO treatment (n=5). (H) Western blotting for the protein expression of pTyr216-GSK-3β in podocytes in high or normal glucose, with and without BIO treatment. Each bar represents mean ± SEM (n=5). 1-4: 1, normal glucose without BIO; 2, normal glucose with BIO; 3, high glucose without BIO; 4, high glucose with BIO. $^{*}$P<0.05 vs. NC group or podocytes in normal glucose group without BIO treatment; $^{\#}$P<0.05, vs. 12-week-old mice in DN group or podocytes in high glucose group without BIO treatment; $^{\Delta}$P<0.05, vs. 12-week-old mice in DN+BIO group. All data are presented as the mean ± standard error of the mean. GSK-3β, glycogen synthase kinase 3β; NC, normal control group (db/+); DN, diabetic neuropathy group (db/db); BIO, (2'Z, 3'E)-6-bromoindirubin-3'-oxime.

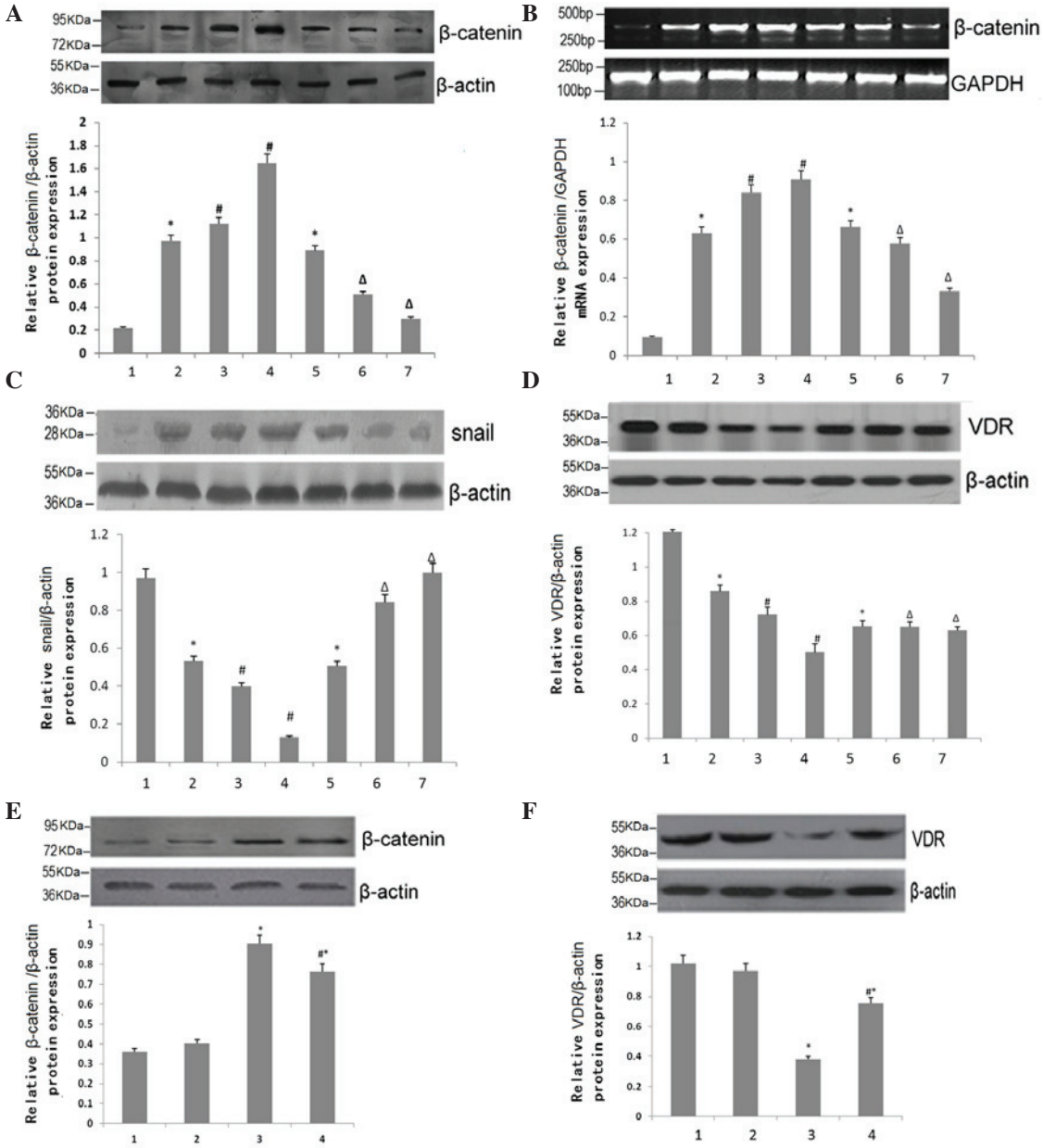


Figure 6. Effects of BIO on the expression levels of β-catenin, Snail and VDR. (A) Western blotting for the protein expression of β-catenin in the kidneys of NC, DN and DN+BIO mice. Data are presented as the mean ± standard error of the mean (n=6). (B) Reverse transcription-quantitative polymerase chain reaction analysis of the mRNA expression of β-catenin in the kidneys of NC, DN and DN+BIO mice. Data are presented as the mean ± standard error of the mean (n=6). (C) Western blotting for the protein expression of Snail expression in the kidneys of NC, DN and DN+BIO mice. Data are presented as the mean ± standard error of the mean (n=4). (D) Western blotting for the protein expression of VDR in the kidneys of NC, DN and DN+BIO mice. Data are presented as the mean ± standard error of the mean (n=6). 1, NC group; 2, DN group; 3, 15 week DN group; 4, 18 week DN group; 5, 12 week BIO group; 6, 15 week BIO group; 7, 18 week BIO group. (E) Western blotting for the protein expression of β-catenin in podocytes in high or normal glucose, with and without BIO treatment. Data are presented as the mean ± standard error of the mean (n=5). (F) Western blotting for the protein expression of VDR in podocytes in high or normal glucose, with and without BIO treatment. 1-4: 1, normal glucose without BIO; 2, normal glucose with BIO; 3, high glucose without BIO; 4, high glucose with BIO. *P<0.05, vs. mice in NC group or podocytes in normal glucose group without BIO treatment; #P<0.05, vs. 12-week-old mice in DN group, or podocytes in high glucose group without BIO treatment; ΔP<0.05, vs.12-week-old mice in DN+BIO group. VDR, vitamin D receptor; NC, normal control group (db/+); DN, diabetic neuropathy group (db/db); BIO, (2'Z, 3'E)-6-bromoindirubin-3'-oxime.

the observations in the protein levels (P<0.05; Fig. 5B). The expression levels of pSer-9-GSK-3β increased significantly at 15 and 18 weeks in the BIO group (P<0.05; Fig. 5C), whereas the patterns observed in the expression of pTyr-216-GSK-3β were similar to those of total-GSK-3β (P<0.05; Fig. 5D). To confirm these observations, the kinase activity of GSK-3β was assessed using a kinase assay to determine the glomerular activity of GSK-3β (Fig. 5E). The activity of GSK-3β in the DN group increased with disease progression, in a time-dependent manner (P<0.05). Following treatment with BIO, the activity of GSK-3β decreased by 15 weeks, and continued to decline until of 18 weeks of age (P<0.05).

The expression of total-GSK-3β in podocytes was also assessed, using RT-qPCR with β-actin as an internal reference (Fig. 5F). Under conditions of high glucose, the expression of total-GSK-3β increased significantly, compared with

normal glucose (P<0.05). Treatment with BIO partially alleviated the high glucose-mediated increases in total-GSK-3β (P<0.05). Similar patterns of expression were observed for pTyr216-GSK-3β in the podocytes, whereas, consistent with previous observations, the protein expression patterns of pSer9-GSK-3β were reversed (P<0.05; Figs. 5G and H).

*Effects of BIO on the expression levels of β-catenin, Snail and VDR*. The expression levels of β-catenin in the mouse kidney tissues were compared, with β-actin as a loading control, using RT-qPCR (Fig. 6A). As DN progressed, the expression of β-catenin in the DN group increased significantly, in a time-dependent matter (Fig. 6A). However, the levels were substantially attenuated by BIO treatment at 15 and 18 weeks of age, compared with the DN group. RT-qPCR analysis of β-catenin in the kidney tissues of the 15-week-old mice confirmed these observations (Fig. 6B). Similar expression patterns for Snail were observed (Fig. 6C). However, the opposite patterns of expression were observed for VDR (P<0.05; Fig. 5D).

The expression of β-catenin in podocytes was also assessed and compared with β-actin, as a loading control, using RT-qPCR (Fig. 6E). Under normal glucose conditions, BIO treatment had no effect (P>0.05). However, under high-glucose conditions, the expression of β-catenin increased significantly, compared with the normal glucose group (P<0.05). Treatment with BIO partially attenuated the high glucose-induced increase in the expression of β-catenin (P<0.05). Consistent with the data from the mouse kidney tissues, the protein expression patterns of VDR in the podocytes were the reverse (Fig. 6F).

## Discussion

*Selection and establishment of animal models*. db/db mice are one of the most commonly used animal models in studies investigating type II diabetes (25). The mouse contains a G>T point mutation in the leptin receptor (LepRdb/db), leading to its aberrant splicing derived by fat cells, and the formation of defective receptors (26,27). As a result, mice overeat, causing symptoms including obesity, hyperinsulinemia and insulin resistance. In addition, db/db mice develop progressive nephrotic disease, making the model suitable for long-term investigations.

The LepRdb/db mutation has been verified in C57BLKS/J (28), C57BL/6J (29) and FVB/NJ strains. The blood glucose levels of male C57BLKS/J db/db mice gradually increases from ~4 weeks of age, and hyperglycemia appears at ~8 weeks (>16 mmol/l). Microalbuminuria occurs at ~10-12 weeks (30-32), with morphological changes, including glomerular hypertrophy, basement membrane thickening, mesangial widening and foot process fusion (33) observed from 12-14 weeks of age. Finally, blood glucose levels peak at ~16 weeks (34-37). Therefore, the present study used male db/db C57BLKS/J mice to establish a model of DN.

The characteristics of the DN model used in the present study were as follows: i) at 12 weeks-of-age, mice exhibited significant polyuria, polydipsia and polyphagia, whereas body weight was 29.91±4.71 g and kidney weight was 180.00±25.66 mg, all of which were significantly different, compared with the NC group (P<0.05). ii) By 12 weeks of age, the blood glucose level in the DN mice was 27.5000±7.78 mmol/l and protein was detected in the urine. These observations were significantly different, compared with the NC group (P<0.05). iii) UAE over a 24 h period in the DN model mice was 239.24±37.80 $\mu$g at 12 weeks of age, which was also significantly different from that in the NC group (P<0.05). Finally, histopathological examination of the kidneys from the DN mice at 12 weeks of age revealed glomerular hypertrophy, basement membrane thickening and mesangial area widening, all of which increased in severity with disease progression. By 18 weeks of age, certain glomeruli exhibited lobulated sclerosis, a characteristic of DN mesangial cells, and capillary endothelial cells. Podocytes, which are glomerular epithelial cells attached to the outside of the GBM, constitute the glomerular filtration barrier between the GBM and capillary endothelium. Podocyte processes protrude from podocyte cell bodies, covering the outer surface of the GBM, and interacting with the GBM via proteoglycan adhesion molecules (38,39). The slit diaphragm, a zipper-like structure situated between two adjacent podocytes, is the final barrier of plasma protein filtration (35). Podocyte injury is involved in the progression of glomerulonephritis, DN, renal failure and other kidney diseases (40). Specifically, reductions in the number and density of podocytes have been linked to the pathological changes, which occur during DN (41). It has been suggested that podocyte phenotypic transformation, the process of its transdifferentiation into mesenchymal cells during cell damage, leads to the loss of specific podocyte protein markers, disrupted cell function and proteinuria (42).

Podocytes are highly differentiated epithelial cells. Several mature protein markers, including nephrin (43), podocin (44) and synaptopodin (45), are found on the surface and slit diaphragms of podocytes, and constitute a charge barrier of the GBM. They are also involved in cell-cell connections and signal transduction, and can maintain the integrity of podocyte foot processes and the normal function of the membrane hole (38,39). Phenotypic markers of mesenchymal cells include α-SMA and fibronectin, which are important for cellular activation and transdifferentiation.

A previous study has revealed that elevated blood glucose can cause mice to produce increased levels of fibronectin and laminin β1 in the extracellular matrix (46). In addition, Kang *et al* revealed that glucose levels can be raised following the induction of the expression of ILK, inducing podocyte transdifferentiation and injury (47).

*Selection and application of treatments for DN*. Clinically, DN treatment includes regulating blood glucose, controlling blood lipids and diet adjustment (48). Frequently used medications include angiotensin-converting enzyme inhibitors and angiotensin receptor blockers (49). However, these therapies only delay the development of ESRD, and do not effectively prevent the development of DN (50-52). GSK-3β is a serine/threonine kinase, which is expressed in all eukaryotic cells. The key amino acids for regulating GSK-3β activity are Tyr-216 for activation and Ser-9 for inhibition. Studies have shown that GSK-3β not only phosphorylates glycogen synthase to regulate the activity of glycolytic enzymes, but is also involved in signaling pathways, including insulin, Hedgehog, Notch and Wnt/β-catenin, to affect cellular differentiation, metabolism and apoptosis (53). During insulin signaling, the

insulin receptor phosphorylates GSK-3β, leading to decreased GSK-3β activity in liver and muscle. This leads to reduced blood glucose levels and an increase in glycogen synthesis. In the Wnt pathway, GSK-3β, β-catenin, adenomatosis polyposis coli and Axin form a complex in the cytoplasm, leading to the degradation of β-catenin by the proteasome and the inhibition of Wnt gene transcription (54). Snail is a zinc finger transcription factor, which can transform epithelial cells into mesenchymal cells. GSK-3β can regulate the expression and activity of Snail, thereby regulating EMT (55,56). Therefore, the present study used BIO, an inhibitor of GSK-3β, to assess the effects of the expression and activity of GSK-3β on the progression of DN.

*Effects of BIO on the development of diabetic nephropathy in db/db mice*. In the present study, the db/db mice, as a model of DN, were treated with the GSK-3β inhibitor, BIO, and the effects on DN progression were assessed. At 18 weeks of age, the symptoms of the mice in BIO group, including polyuria, polydipsia and polyphagia, were significantly reduced. In addition, body weight was 32.49±4.77 g and kidney weight was 159.90±22.53 mg, which were significantly different, compared with those in the DN group ($P<0.05$). By 18 weeks of age, the blood glucose level in the BIO group was 28.7625±2.71 mmol/l, which was comparable to that in the DN group, suggesting that BIO had no effect on blood glucose ($P>0.05$). The UAE of mice in BIO group was 135.65±18.96 $\mu$g over 24 h, which was decreased significantly from the DN group ($P<0.05$). At ~18 weeks of age, renal pathological lesions, including mesangial cell proliferation and matrix, increased significantly in the DN group, but were alleviated by treatment with BIO. These data suggested that the GSK-3β inhibitor reduced proteinuria and slowed the progression of early DN. Of note, the mechanism underlying this protection of the kidney may involve adjusting EMT, but not lowering blood glucose.

*Effects of BIO on GSK-3β in the db/db mouse kidney*. Normal kidney tissue expresses small quantities of total-GSK-3β, however protein and mRNA expression levels were observed to increase with the progression of DN, in a time-dependent manner ($P<0.05$). Following treatment with BIO, the upregulation of total-GSK-3β was lower, compared with the control group ($P<0.05$). Similar expression patterns were observed for Tyr216-phosphorylated GSK-3β (pTyr216-GSK-3β) were observed. By contrast, Ser-9 phosphorylated GSK-3β (pSer9-GSK-3β) was expressed at a high level in normal renal tissues, but decreased with the development of DN, in a time-dependent manner ($P<0.05$). Following treatment with BIO, the levels of pSer9-GSK-3β were reduced, compared with the DN group ($P<0.05$). With the progression of DN, GSK-3β kinase activity in the DN group increased in a time-dependent matter, whereas treatment with BIO for 3 weeks led to a partial decrease in GSK-3β kinase activity, compared with the DN group. Following 6 weeks of BIO therapy, the activity of GSK-3β was further reduced ($P<0.05$). These results suggested that BIO, an inhibitor of GSK-3β, effectively affected the activity of GSK-3β, and may be useful for the treatment of DN.

*Effects of BIO on EMT in the db/db mouse kidney*. In the present study, as EMT developed in the renal cortex of mice in the DN group, the expression levels of total GSK-3β and pTyr216-GSK-3β, and the activity of GSK-3β all increased, whereas the levels of pSer9-GSK-3β declined. Therefore, it was hypothesized that the activation of GSK-3β is important in EMT, and that inhibiting the activity of GSK-3β may delay the development of EMT.

BIO was used to inhibit the activation of GSK-3β in the DN mice. When the mice were treated with BIO, the protein and mRNA expression levels of epithelial phenotype markers, including podocin, podocin and synaptopodin, increased in a time-dependent manner, which was significantly different, compared with the DN group ($P<0.05$). In addition, the expression levels of mesenchymal markers, including fibronectin and α-SMA, were decreased significantly, compared with those in the DN group ($P<0.05$). These results suggested that BIO, effectively reduced EMT in the db/db mice with DN.

During Wnt signaling, the upregulation of GSK-3β activity can lead to degradation of β-catenin (54) and decreased expression of Snail (57,58). Previous studies have revealed that using small interfering (si)RNA against GSK-3β can cause transdifferentiation of mammary gland tissue and skin epithelial cells (59). In addition, the activity of GSK-3β may maintain the structure of epithelial cells and their surface role in the normal podocyte phenotype (60,61). In contrast with these data, the present study revealed that normal kidney tissue expressed low levels of β-catenin and Snail. During the progression of DN, the expression levels of β-catenin and Snail increased, and the activity of GSK-3β was also upregulated in a time-dependent manner ($P<0.05$). Following treatment with BIO, the upregulation in the levels of β-catenin and Snail were inhibited significantly, compared with those in the DN group ($P<0.05$). These observations contradict previous observations in traditional Wnt signaling (62). It has been suggested that the activation of GSK-3β may directly stimulate transdifferentiation by triggering the transcription of relevant genes, and inhibiting the expression of epithelial cell markers (63). In the resting state, β-catenin is bound to fibronectin, which anchors in the cell membrane. This causes transdifferentiation of epithelial cells, following which β-catenin dissociates and migrates to the cytoplasm. Intracellular β-catenin then tends to migrate towards the nucleus (64), further promoting the transcription of transdifferentiation-associated genes.

Abnormalities in the expression of vitamin D are frequently observed in patients with chronic kidney disease (65). VDR, a receptor specific for vitamin D, has a protective effect in the kidneys, and its expression in the renal tissues of patients with DN is decreased (66). Once activated, VDR specifically combines with the DNA structural domain of vitamin D, and undergoes conformational change allowing it to combine with specific DNA regions. This leads to novel gene expression, resulting in a series of biological effects. In a previous study on human bone marrow stromal cells, the 1, 25 (OH)-2-vitamin D3 system activated VDR, which then combined with β-catenin in the nucleus, leading to the transport of β-catenin out of the nucleus (67). When activated by its ligand, VDR competitively combines with T cell transcription factor-4, which is normally bound to β-catenin, thus inhibiting the activity of β-catenin in colon cancer (68). In a mouse model of unilateral ureteral obstruction, it was observed that VDR was associated with the extent and development of renal fibrosis. Loss of the expression

of VDR caused epithelial cell transdifferentiation, which may be mediated by β-catenin. Specifically, when the cells were treated with VDR siRNA, the expression of β-catenin was increased and transported to the nucleus, whereas the over-expression of VDR inhibited the expression of β-catenin (69). The data presented in the present study demonstrated that the expression of VDR was decreased in the DN group, and the levels of β-catenin and Snail were increased. As expected, these changes were ameliorated following treatment with BIO, suggesting that GSK-3β may modulate the expression levels of β-catenin and Snail by regulating the expression of VDR. Therefore, the present study hypothesized that GSK-3β uses pathways in addition to the classical Wnt pathway to regulate and control EMT. This may explain why the activation of GSK-3β increased, and treatment with the GSK-3β inhibitor decreased, the expression levels of β-catenin and Snail, which were observations contradictory to the classical Wnt pathway.

*Advantages and disadvantages of the clinical application of GSK-3β inhibitors*. GSK-3β is a multifunctional protein, which is involved in several biological processes, including the transdifferentiation, proliferation, apoptosis and migration of several different cell types. During the transdifferentiation of renal tubular epithelial cells induced by high glucose, reports on GSK-3β activity are conflicting. It has been suggested that GSK-3β activity is reduced during the transdifferentiation of renal tubular epithelial cells induced by high glucose (70), whereas other have suggested that the activity of GSK-3β increases during high-glucose-mediated apoptosis in mesangial cells (71). In addition, studies have reported that the expression of GSK-3β increases in patients with type 2 diabetes and in rodent models of obesity and insulin resistance (72,73).

Further investigations are required to clarify the role of GSK-3β in high-glucose-stimulated DN, and specifically to clarify the association between GSK-3β, EMT and DN proteinuria. The data in the present study suggested that BIO, as an inhibitor of GSK-3β, can cause transdifferentiation of podocytes. Additional data suggested that LiCl, another inhibitor of GSK-3β has a similar role in EMT (data not shown) (74). Furthermore, the effects of GSK-3β in podocyte EMT were verified using GSK-3β RNA interference in podocytes, the results of which supported the conclusions of the present study. However, additional investigations are required to define the mechanisms underlying the effects of GSK-3β inhibitors in the treatment of DN, and the downstream signal transduction pathways. In addition, investigations on the long-term treatment with BIO is essential prior to its consideration as a therapeutic agent for the treatment of DN.

In conclusion, the present study demonstrated that, during the development of diabetic nephropathy, the expression levels of glomerular epithelial cell markers decreased, and the levels of mesenchymal-like markers increased in a time-dependent manner, suggesting the occurrence of EMT. In addition, the expression and activity of total-GSK-3β increased, the expression of pSer9-GSK-3β (the inhibitory site of GSK-3β) decreased and the expression of pTyr216-GSK-3β (the active site of GSK-3β) increased. This suggested that the activity of GSK-3β is closely associated with the development of DN in db/db mice. Following treatment with BIO, the expression of kidney epithelial cell markers in mice with DN increased, whereas the expression of mesenchymal-like markers decreased, compared with the untreated DN mice, suggesting that the inhibitor of GSK-3β partially reversed EMT. The present study also demonstrated that treatment with BIO reduced proteinuria leakage, delayed the deterioration of renal function and prevented structural changes in the kidneys of the mice with DN. This suggested that GSK-3β may regulate podocyte EMT, and that the GSK-3β inhibitor, BIO, may protect the filtration barrier of the glomerulus, reversing EMT and delaying the development of DN.

The present study also observed that the activation of GSK-3β increased the expression levels of β-catenin and Snail. Following GSK-3β inhibition by BIO, the expression levels of β-catenin and snail decreased. These effects may be due to the fact that EMT is directly associated with GSK-3β activity, which may inhibit the gene transcription of epithelial cell marker proteins. When EMT occurs, β-catenin dissociates from the cytomembrane and translocates to the cytoplasm, increased concentrations of intracellular β-catenin migrate and accumulate in the nucleus, accelerating the transcription of transdifferentiation-associated genes. In addition, it is possible that GSK-3β regulated the expression of VDR, and was consequently involved in regulating the expression of β-catenin and Snail. Therefore, the present study hypothesized that, rather than relying on the classical Wnt pathway to control EMT, GSK-3β can also regulate podocytes by modifying the levels of VDR, or by stimulating the nuclear accumulation of β-catenin.

## Acknowledgements

The authors would like to thank Dr Li-Bin Zhang (Basic Medical College, Xinxiang Medical University) for discussion, and Dr Xin-Lai Qian (The Third Affiliated Hospital of Xinxiang Medical University, Xinxiang, China) and Dr Song-Xia Quan (The First Affiliated Hospital of Zhengzhou University) for their invaluable assistance in histological analyses. The authors would also like to thank Dr Ying Zhao (Department of Foreign Language, Henan Institute of Science and Technology, Zhengzhou, China) and Dr Peng Wan (Henan Time Culture Media Company, Zhengzhou, China) for their editorial assistance. This study was supported by grants from the National Basic Research Program of China 973 Program (grant nos, 2012CB517600 and 2012CB517606) and the National Natural Science Foundation of China (grant nos. 81070574 and 81270807).

## References

1. US Renal Data System: 2009 USRDS Annual Data Report: Epidemiology of kidney disease in the United States. National Institutes of Health, National Institute of Diabetes and Digestive and Kidney Diseases, Bethesda, MD, 2009.
2. de Boer IH, Rue TC, Hall YN, Heagerty PJ, Weiss NS and Himmelfarb J: Temporal trends in the prevalence of diabetic kidney disease in the United States. JAMA 305: 2532-2539, 2011.
3. Panchapakesan U, Pegg K, Gross S, Komala MG, Mudaliar H, Forbes J, Pollock C and Mather A: Effects of SGLT2 inhibition in human kidney proximal tubular cells-renoprotection in diabetic nephropathy? PLoS One 8: e54442, 2013.
4. Dronavalli S, Duka I and Bakris GL: The pathogenesis of diabetic nephropathy. Nat Clin Pract Endocrinol Metab 4: 444-452, 2008.
5. Kanwar YS, Wada J, Sun L, Xie P, Wallner EI, Chen S, Chugh S and Danesh FR: Diabetic nephropathy: Mechanisms of renal disease progression. Exp Biol Med (Maywood) 233: 4-11, 2008.

6. Wolf G and Ziyadeh FN: Molecular mechanisms of diabetic renal hypertrophy. Kidney Int 56: 393-405, 1999.
7. Wolf G and Ziyadeh FN: Cellular and molecular mechanisms of proteinuria in diabetic nephropathy. Nephron Physiol 106: p26-p31, 2007.
8. Lomelí C, Rosas-Peralta M, Lorenzo A and Saucedo N; Grupo de investigadores participantes en México para el estudio I-Search: Microalbuminuria and associated cardiovascular risk factors in patients with arterial systemic hypertension. A subanalysis of the I-Search study. Arch Cardiol Mex 82: 93-104, 2012 (In Spanish).
9. Monhart V: Microalbuminuria. From diabetes to cardiovascular risk. Vnitr Lek 57: 293-298, 2011 (In Czech).
10. Ozyol A, Yucel O, Ege MR, Zorlu A and Yilmaz MB: Microalbuminuria is associated with the severity of coronary artery disease independently of other cardiovascular risk factors. Angiology 63: 457-460, 2012.
11. Udenze IC, Azinge EC, Ebuehi OA, Awolola NA, Adekola OO, Menkiti I and Irurhe NK: The relationship between microalbuminuria, cardiovascular risk factors and disease management in type 2 diabetes. Nig Q J Hosp Med 22: 34-38, 2012.
12. Harris RC: Podocyte ACE2 protects against diabetic nephropathy. Kidney Int 82: 255-256, 2012.
13. Wiggins RC: The spectrum of podocytopathies: A unifying view of glomerular diseases. Kidney Int 71: 1205-1214, 2007.
14. Reidy K and Susztak K: Epithelial-mesenchymal transition and podocyte loss in diabetic kidney disease. Am J Kidney Dis 54: 590-593, 2009.
15. Steffes MW, Schmidt D, McCrery R and Basgen JM; International Diabetic Nephropathy Study Group: Glomerular cell number in normal subjects and in type 1 diabetic patients. Kidney Int 59: 2104-2113, 2001.
16. Susztak K, Raff AC, Schiffer M and Böttinger EP: Glucose-induced reactive oxygen species cause apoptosis of podocytes and podocyte depletion at the onset of diabetic nephropathy. Diabetes 55: 225-233, 2006.
17. Thibodeau JF, Holterman CE, Burger D, Read NC, Reudelhuber TL and Kennedy CR: A novel mouse model of advanced diabetic kidney disease. PLoS One 9: e113459, 2014.
18. Hu P, Wang G, Shen M, Zhang P, Zhang J, Du J and Liu Q: Intratumoral polymorphonuclear granulocyte is associated with poor prognosis in squamous esophageal cancer by promoting epithelial-mesenchymal transition. Future Oncol 11: 771-783, 2015.
19. Dai HY, Zheng M, Lv LL, Tang RN, Ma KL, Liu D, Wu M and Liu BC: The roles of connective tissue growth factor and integrin-linked kinase in high glucose-induced phenotypic alterations of podocytes. J Cell Biochem 113: 293-301, 2012.
20. Liang Y, Jing Z, Deng H, Li Z, Zhuang Z, Wang S and Wang Y: Soluble epoxide hydrolase inhibition ameliorates proteinuria-induced epithelial-mesenchymal transition by regulating the PI3K-Akt-GSK-3β signaling pathway. Biochem Biophys Res Commun 463: 70-75, 2015.
21. Obligado SH, Ibraghimov-Beskrovnaya O, Zuk A, Meijer L and Nelson PJ: CDK/GSK-3 inhibitors as therapeutic agents for parenchymal renal diseases. Kidney Int 73: 684-690, 2008.
22. Mundel P, Reiser J, Zúñiga Mejía Borja A, Pavenstädt H, Davidson GR, Kriz W and Zeller R: Rearrangements of the cytoskeleton and cell contacts induce process formation during differentiation of conditionally immortalized mouse podocyte cell lines. Exp Cell Res 236: 248-258, 1997.
23. Dai C, Stolz DB, Kiss LP, Monga SP, Holzman LB and Liu Y: Wnt/beta-catenin signaling promotes podocyte dysfunction and albuminuria. J Am Soc Nephrol 20: 1997-2008, 2009.
24. Jonathan Ryves W, Dalton EC, Harwood AJ and Williams RS: GSK-3 activity in neocortical cells is inhibited by lithium but not carbamazepine or valproic acid. Bipolar Disord 7: 260-265, 2005.
25. Hummel KP, Dickie MM and Coleman DL: Diabetes, a new mutation in the mouse. Science 153: 1127-1128, 1966.
26. Chen H, Charlat O, Tartaglia LA, Woolf EA, Weng X, Ellis SJ, Lakey ND, Culpepper J, Moore KJ, Breitbart RE, *et al*: Evidence that the diabetes gene encodes the leptin receptor: Identification of a mutation in the leptin receptor gene in db/db mice. Cell 84: 491-495, 1996.
27. Lee GH, Proenca R, Montez JM, Carroll KM, Darvishzadeh JG, Lee JI and Friedman JM: Abnormal splicing of the leptin receptor in diabetic mice. Nature 379: 632-635, 1996.
28. Hummel KP, Coleman DL and Lane PW: The influence of genetic background on expression of mutations at the diabetes locus in the mouse. I. C57BL-KsJ and C57BL-6J strains. Biochem Genet 7: 1-13, 1972.
29. Chua S Jr, Liu SM, Li Q, Yang L, Thassanapaff VT and Fisher P: Differential beta cell responses to hyperglycaemia and insulin resistance in two novel congenic strains of diabetes (FVB- Lepr (db)) and obese (DBA-Lep (ob)) mice. Diabetologia 45: 976-990, 2002.
30. Cohen MP, Clements RS, Cohen JA and Shearman CW: Prevention of decline in renal function in the diabetic db/db mouse. Diabetologia 39: 270-274, 1996.
31. Lim AK, Ma FY, Nikolic-Paterson DJ, Thomas MC, Hurst LA and Tesch GH: Antibody blockade of c-fms suppresses the progression of inflammation and injury in early diabetic nephropathy in obese db/db mice. Diabetologia 52: 1669-1679, 2009.
32. Chow FY, Nikolic-Paterson DJ, Ozols E, Atkins RC and Tesch GH: Intercellular adhesion molecule-1 deficiency is protective against nephropathy in type 2 diabetic db/db mice. J Am Soc Nephrol 16: 1711-1722, 2005.
33. Chodavarapu H, Grobe N, Somineni HK, Salem ES, Madhu M and Elased KM: Rosiglitazone treatment of type 2 diabetic db/db mice attenuates urinary albumin and angiotensin converting enzyme 2 excretion. PLoS One 8: e62833, 2013.
34. Vivanco I and Sawyers CL: The phosphatidylinositol 3-Kinase AKT pathway in human cancer. Nat Rev Cancer 2: 489-501, 2002.
35. Ward SG and Finan P: Isoform-specific phosphoinositide 3-kinase inhibitors as therapeutic agents. Curr Opin Pharmacol 3: 426-434, 2003.
36. Franke TF, Hornik CP, Segev L, Shostak GA and Sugimoto C: PI3 K/Akt and apoptosis: Size matters. Oncogene 22: 8983-8998, 2003.
37. Chua S Jr, Li Y, Liu SM, Liu R, Chan KT, Martino J, Zheng Z, Susztak K, D'Agati VD and Gharavi AG: A susceptibility gene for kidney disease in an obese mouse model of type II diabetes maps to chromosome 8. Kidney Int 78: 453-462, 2010.
38. Taneda S, Honda K, Ohno M, Uchida K, Nitta K and Oda H: Podocyte and endothelial injury in focal segmental glomerulosclerosis: An ultrastructural analysis. Virchows Arch 467: 449-458, 2015.
39. Lenoir O, Jasiek M, Hénique C, Guyonnet L, Hartleben B, Bork T, Chipont A, Flosseau K, Bensaada I, Schmitt A, *et al*: Endothelial cell and podocyte autophagy synergistically protect from diabetes-induced glomerulosclerosis. Autophagy 11: 1130-1145, 2015.
40. Dai C, Stolz DB, Bastacky SI, St-Arnaud R, Wu C, Dedhar S and Liu Y: Essential role of integrin-linked kinase in podocyte biology: Bridging the integrin and slit diaphragm signaling. J Am Soc Nephrol 17: 2164-2175, 2006.
41. Xu W, Chen J, Lin J, Liu D, Mo L, Pan W, Feng J, Wu W and Zheng D: Exogenous H2S protects H9c2 cardiac cells against high glucose-induced injury and inflammation by inhibiting the activation of the NF-κB and IL-1β pathways. Int J Mol Med 35: 177-186, 2015.
42. El-Aouni C, Herbach N, Blattner SM, Henger A, Rastaldi MP, Jarad G, Miner JH, Moeller MJ, St-Arnaud R, Dedhar S, *et al*: Podocyte-specific deletion of integrin-linked kinase results in severe glomerular basement membrane alterations and progressive glomerulosclerosis. J Am Soc Nephrol 17: 1334-1344, 2006.
43. Langham RG, Kelly DJ, Cox AJ, Thomson NM, Holthöfer H, Zaoui P, Pinel N, Cordonnier DJ and Gilbert RE: Proteinuria and the expression of the podocyte slit diaphragm protein, nephrin, in diabetic nephropathy: Effects of angiotensin converting enzyme inhibition. Diabetologia 45: 1572-1576, 2002.
44. Nakatsue T, Koike H, Han GD, Suzuki K, Miyauchi N, Yuan H, Salant DJ, Gejyo F, Shimizu F and Kawachi H: Nephrin and podocin dissociate at the onset of proteinuria in experimental membranous nephropathy. Kidney Int 67: 2239-2253, 2005.
45. Mundel P, Heid HW, Mundel TM, Krüger M, Reiser J and Kriz W: Synaptopodin: An actin-associated protein in telencephalic dendrites and renal podocytes. J Cell Biol 139: 193-204, 1997.
46. Liu W, Hu M, Wang Y, Sun B, Guo Y, Xu Z, Li J and Han B: Overexpression of interleukin-18 protein reduces viability and induces apoptosis of tongue squamous cell carcinoma cells by activation of glycogen synthase kinase-3β signaling. Oncol Rep 33: 1049-1056, 2015.
47. Kang YS, Li Y, Dai C, Kiss LP, Wu C and Liu Y: Inhibition of integrin-linked kinase blocks podocyte epithelial-mesenchymal transition and ameliorates proteinuria. Kidney Int 78: 363-373, 2010.

48. Cai X, Han X, Luo Y and Ji L: Analysis of insulin doses of Chinese type 2 diabetic patients with intensive insulin treatment. PLoS One 7: e38962, 2012.
49. Tang L, Yi R, Yang B, Li H, Chen H and Liu Z: Valsartan inhibited HIF-1α pathway and attenuated renal interstitial fibrosis in streptozotocin-diabetic rats. Diabetes Res Clin Pract 97: 125-131, 2012.
50. Berwick DC, Hers I, Heesom KJ, Moule SK and Tavare JM: The identification of ATP-citrate lyase as a protein kinase B (Akt) substrate in primary adipocytes. J Biol Chem 277: 33895-33900, 2002.
51. Brunet A, Bonni A, Zigmond MJ, Lin MZ, Juo P, Hu LS, Anderson MJ, Arden KC, Blenis J and Greenberg ME: Akt promotes cell survival by phosphorylating and inhibiting a Forkhead transcription factor. Cell 96: 857-868, 1999.
52. Figueroa C, Tarras S, Taylor J and Vojtek AB: Akt2 negatively regulates assembly of the POSH-MLK-JNK signaling complex. J Biol Chem 278: 47922-47927, 2003.
53. Kim WY and Snider WD: Functions of GSK-3 Signaling in development of the nervous system. Front Mol Neurosci 4: 44, 2011.
54. Lee J and Kim MS: The role of GSK3 in glucose homeostasis and the development of insulin resistance. Diabetes Res Clin Pract 77 (Suppl 1): S49-S57, 2007.
55. Yoshino J, Monkawa T, Tsuji M, Inukai M, Itoh H and Hayashi M: Snail1 is involved in the renal epithelial-mesenchymal transition. Biochem Biophys Res Commun 362: 63-68, 2007.
56. Bachelder RE, Yoon SO, Franci C, de Herreros AG and Mercurio AM: Glycogen synthase kinase-3 is an endogenous inhibitor of Snail transcription: Implications for the epithelial-mesenchymal transition. J Cell Biol 168: 29-33, 2005.
57. Jiang J and Griffin JD: Wnt/β-catenin pathway modulates the sensitivity of the mutant flt3 receptor kinase inhibitors in a GSK-3β dependent manner. Genes Cancer 1: 164-176, 2010.
58. Zhou BP, Deng J, Xia W, Xu J, Li YM, Gunduz M and Hung MC: Dual regulation of Snail by GSK-3beta-mediated phosphorylation in control of epithelial-mesenchymal transition. Nat Cell Biol 6: 931-940, 2004.
59. Wang Y, Feng W, Xue W, Tan Y, Hein DW, Li XK and Cai L: Inactivation of GSK-3beta by metallothionein prevents diabetes-related changes in cardiac energy metabolism, inflammation, nitrosative damage and remodeling. Diabetes 58: 1391-1402, 2009.
60. Shi WR, Liu Y, Xie JD, Zhuo S, Tu CX and Xie ZF: Changes in Wnt pathway inhibiting factors in nitrosamine-induced esophageal precancerosis lesions and effect of gexia zhuyu decoction. Zhongguo Zhong Yao Za Zhi 39: 3131-3135, 2014 (In Chinese).
61. Mariappan MM, Shetty M, Sataranatarajan K, Choudhury GG and Kasinath BS: Glycogen synthase kinase 3beta is a novel regulator of high glucose- and high insulin-induced extracellular matrix protein synthesis in renal proximal tubular epithelial cells. J Biol Chem 283: 30566-30575, 2008.
62. Yao CJ, Lai GM, Yeh CT, Lai MT, Shih PH, Chao WJ, Whang-Peng J, Chuang SE and Lai TY: Honokiol eliminates human oral cancer stem-like cells accompanied with suppression of Wnt/β-catenin signaling and apoptosis induction. Evid Based Complement Alternat Med 2013: 146136, 2013.
63. Li Y, Kang YS, Dai C, Kiss LP, Wen X and Liu Y: Epithelial-to-mesenchymal transition is a potential pathway leading to podocyte dysfunction and proteinuria. Am J Pathol 172: 299-308, 2008.
64. Solanas G, Porta-de-la-Riva M, Agustí C, Casagolda D, Sánchez-Aguilera F, Larriba MJ, Pons F, Peiró S, Escrivà M, Muñoz A, *et al*: E-cadherin controls beta-catenin and NF-kappaB transcriptional activity in mesenchymal gene expression. J Cell Sci 121: 2224-2234, 2008.
65. Cozzolino M, Brenna I, Volpi E, Ciceri P, Mehmeti F and Cusi D: Restoring the physiology of vitamin D receptor activation and the concept of selectivity. Contrib Nephrol 171: 151-156, 2011.
66. Zhang Y, Deb DK, Kong J, Ning G, Wang Y, Li G, Chen Y, Zhang Z, Strugnell S, Sabbagh Y, *et al*: Long-term therapeutic effect of vitamin D analog doxercalciferol on diabetic nephropathy: Strong synergism with AT1 receptor antagonist. Am J Physiol Renal Physiol 297: F791-F801, 2009.
67. Fretz JA, Zella LA, Kim S, Shevde NK and Pike JW: 1, 25-Dihydroxyvitamin D3 regulates the expression of low-density lipoprotein receptor-related protein 5 via deoxyribonucleic acid sequence elements located downstream of the start site of transcription. Mol Endocrinol 20: 2215-2230, 2006.
68. Rincon-Choles H, Vasylyeva TL, Pergola PE, Bhandari B, Bhandari K, Zhang JH, Wang W, Gorin Y, Barnes JL and Abboud HE: ZO-1 expression and phosphorylation in diabetic nephropathy. Diabetes 55: 894-900, 2006.
69. Xiong M, Gong J, Liu Y, Xiang R and Tan X: Loss of vitamin D receptor in chronic kidney disease: A potential mechanism linking inflammation to epithelial-to-mesenchymal transition. Am J Physiol Renal Physiol 303: F1107-F1115, 2012.
70. Song H, Deng B, Zou C, Huai W, Zhao R and Zhao W: GSK3β negatively regulates LPS-induced osteopontin expression via inhibiting its transcription. Scand J Immunol 81: 186-191, 2015.
71. Liu Y: New insights into epithelial-mesenchymal transition in kidney fibrosis. J Am Soc Nephrol 21: 212-222, 2010.
72. Jope RS, Yuskaitis CJ and Beurel E: Glycogen synthase kinase-3 (GSK3): Inflammation, diseases and therapeutics. Neurochem Res 32: 577-595, 2007.
73. Lin CL, Wang JY, Huang YT, Kuo YH, Surendran K and Wang FS: Wnt/beta-catenin signaling modulates survival of high glucose-stressed mesangial cells. J Am Soc Nephrol 17: 2812-2820, 2006.
74. Costabile V, Duraturo F, Delrio P, Rega D, Pace U, Liccardo R, Rossi GB, Genesio R, Nitsch L, Izzo P and de Rosa M: Lithium chloride induces mesenchymal-to-epithelial reverting transition in primary colon cancer cell cultures. Int J Oncol 46: 1913-1923, 2015.